

**Title page**

**Title:**

GPR40-mediated  $G\alpha_{12}$  activation by allosteric full agonists highly efficacious at potentiating glucose-stimulated insulin secretion in human islets

**Authors:**

Marie-Laure Rives, Brian Rady, Nadia Swanson, Shuyuan Zhao, Jenson Qi, Eric Arnoult, Ivona Bakaj, Arturo Mancini, Billy Breton, S. Paul Lee, Mark R. Player and Alessandro Pocai

**Affiliations:**

Molecular and Cellular Pharmacology, Janssen Research & Development, LLC, La Jolla, CA 92121, USA (MLR, NS); Cardiovascular and Metabolism, Janssen Research & Development, LLC, Welsh and McKean Roads, Spring House, PA 19477-0776, USA (BR, SZ, JQ, IB, SPL, MRP and AP); Computational Chemistry, Janssen Research & Development, LLC, Welsh and McKean Roads, Spring House, PA 19477-0776, USA (EA) and Domain Therapeutics NA Inc, 7171 Frédérick Banting, Montreal, H4S 1Z9, Quebec, Canada (AM and BB).

**Running title page**

a/ Running title: GPR40 full agonists induce coupling to G $\alpha$ 12

b/ Address correspondence to: Dr. Marie-Laure Rives, Molecular and Cellular Pharmacology  
Janssen, Pharmaceutical companies of Johnson & Johnson, 3210 Merryfield Road, San Diego, CA  
92121, Phone: 858-320-3494

Email: [mrives1@its.jnj.com](mailto:mrives1@its.jnj.com)

c/ Number of text pages: 40

Number of tables: 1

Number of figures: 7

Number of references: 54

Number of words in abstract: 245

Number of words in introduction: 618

Number of words in discussion: 1493

d) List of nonstandard abbreviations: GSIS, Glucose-stimulated insulin secretion; GLP-1, Glucagon-like peptide 1; T2DM, Type-2 Diabetes mellitus; IP1, Inositol-1-phosphate; IP3, D-myo-inositol 1,4,5-triphosphate; PKD, Protein kinase D; GPCR, G protein-coupled receptor; FBS, Fetal bovine serum; PAM, Positive Allosteric Modulator

**ABSTRACT:**

GPR40 is a clinically validated molecular target for the treatment of diabetes. Many GPR40 agonists have been identified to date, with the partial agonist fasiglifam (TAK-875) reaching phase III clinical trials before its development was terminated due to off-target liver toxicity. Since then, attention has shifted toward the development of full agonists that exhibit superior efficacy in preclinical models. Full agonists bind to a distinct binding site, suggesting conformational plasticity and a potential for biased agonism. Indeed, it has been suggested that alternative pharmacology may be required for meaningful efficacy. In this study, we described the discovery and characterization of Compound A, a newly identified GPR40 allosteric full agonist highly efficacious in human islets at potentiating glucose-stimulated insulin secretion. We compared Compound A-induced GPR40 activity to that induced by both fasiglifam and AM-1638, another allosteric full agonist previously reported to be highly efficacious in preclinical models, at a panel of G proteins. Compound A was a full agonist at both the  $G\alpha_q$  and  $G\alpha_i2$  pathways and in contrast to fasiglifam, Compound A also induced  $G\alpha_{12}$  coupling. Compound A and AM-1638 displayed similar activity at all pathways tested. The  $G\alpha_{12}/G\alpha_{13}$ -mediated signaling pathway has been linked to protein kinase D activation as well as actin remodeling, well known to contribute to the release of insulin vesicles. Our data suggest that the pharmacology of GPR40 is complex and that  $G\alpha_{12}/G\alpha_{13}$ -mediated signaling, which may contribute to GPR40 agonists therapeutic efficacy, is a specific property of GPR40 allosteric full agonists.

## **Introduction:**

Activation of the free fatty acid receptor 1 (FFA1), also known as GPR40, potentiates glucose-stimulated insulin secretion (GSIS) from pancreatic  $\beta$ -cells and stimulates the release of incretins, such as glucagon-like peptide 1 (GLP-1) from enteroendocrine cells (Briscoe *et al.*, 2006; Briscoe *et al.*, 2003; Edfalk *et al.*, 2008; Hardy *et al.*, 2005; Itoh *et al.*, 2003; Latour *et al.*, 2007; Luo *et al.*, 2012; Mancini *et al.*, 2013; Shapiro *et al.*, 2005; Stoddart *et al.*, 2008; Tomita *et al.*, 2005; Yonezawa *et al.*, 2004). GLP-1 further promotes GSIS and also decreases hepatic gluconeogenesis, inhibits glucagon secretion, reduces body weight, and improves insulin sensitivity (Baggio *et al.*, 2007; Gorski *et al.*, 2017; Holst, 2007; Pocai, 2012). Thus, the dual mechanisms of GPR40 in pancreatic  $\beta$ -cells as well as in enteroendocrine cells provide considerable rationale for the development of GPR40 agonists for the treatment of type-2 diabetes mellitus (T2DM), with a potential for weight management.

A number of potent, synthetic GPR40 agonists have been reported and a GPR40 partial agonist, fasiglifam from Takeda, advanced as far as phase III clinical trials (Kaku *et al.*, 2015). In a phase II study in T2DM, fasiglifam induced a similar glucose-lowering effect (HbA1c: ca.1%) to that of glimepiride (Burant *et al.*, 2012; Leifke *et al.*, 2012). In spite of similar promising results in Phase III, fasiglifam was withdrawn from development due to drug-induced liver injury (DILI) (Hedrington *et al.*, 2014; Otieno *et al.*, 2017).

Since then, numerous full agonists with superior efficacy both *in vitro* and *in vivo* compared to fasiglifam have been reported (Defossa *et al.*, 2014; Li *et al.*, 2016). Interestingly, these full agonists bind to a recently identified binding site, distinct from previously predicted pockets, and

different from that of endogenous fatty acids and of fasiglifam or other partial agonists (Defossa *et al.*, 2014; Hauge *et al.*, 2015; Lin *et al.*, 2012; Lu *et al.*, 2017; Srivastava *et al.*, 2014). The presence of multiple binding sites suggests conformational plasticity, highlighting a potential for biased agonism (Costa-Neto *et al.*, 2016; Kenakin *et al.*, 2013; Kenakin *et al.*, 2012; Rankovic *et al.*, 2016). GPR40 is mostly known to couple to the heterotrimeric G protein  $G\alpha q/11$  (Shapiro *et al.*, 2005). However, it has also been shown that GPR40 could couple to other pathways in a ligand-dependent manner and that only allosteric full agonists able to induce the activation of such alternative pathways, such as the  $G\alpha s/cAMP$  pathway, could trigger maximal efficacy in preclinical models (Defossa *et al.*, 2014; Hauge *et al.*, 2015; Lin *et al.*, 2012). GPR40 has also been shown to couple to  $G\alpha i/o$  and to arrestin (Mancini *et al.*, 2015; Schroder *et al.*, 2011), and arrestin recruitment has been shown to contribute to GPR40-mediated GSIS (Mancini *et al.*, 2015).

Through a rational design approach, we have identified a new hGPR40 full agonist at the  $G\alpha q/IP1/calcium$  pathway fully efficacious at enhancing GSIS in human islets. We compared Compound A-induced GPR40 activity at a panel of G proteins and to that induced by both fasiglifam as well as AM-1638, previously reported as a highly efficacious hGPR40 allosteric full agonist (Hauge *et al.*, 2015; Li *et al.*, 2016). Our data indicated that Compound A and AM-1638 were both hGPR40 allosteric full agonists, not only at the  $G\alpha q$  pathway but also at  $G\alpha i2$ , with no to very weak efficacy at the  $G\alpha s/cAMP$  pathway. Interestingly, in contrast to fasiglifam and  $\alpha$ -linolenic acid, Compound A and AM-1638 strongly engaged the  $G\alpha 12$  protein. Our data suggest that the pharmacology of GPR40 is complex and that  $G\alpha 12/G\alpha 13$ -mediated signaling, which may contribute to the release of vesicles possibly via protein kinase D (PKD) activation and actin

remodeling, is a specific property of the GPR40 allosteric full agonists Compound A and AM-1638.

## **Materials and Methods**

### *Cell lines and cell culture*

The hGPR40 low-expressing stable CHO-K1 cell line used in this study was purchased from Multispan, Inc (Cat # C1101-1A). The receptor density in this cell line was evaluated by whole cell radioligand saturation binding at  $47,112 \pm 5,088$  receptors per cell, which was comparable to the GPR40 density in a rat insulinoma  $\beta$ -cell line INS-1 832/13 ( $41,519 \pm 9,516$  receptors per cell). Cells were maintained in DMEM/F-12 supplemented with 10% FBS, 1% penicillin/streptomycin and 10  $\mu\text{g/ml}$  puromycin and incubated at 37 °C with 5% CO<sub>2</sub>.

### *IP1 HTRF assay*

The day before the assay, hGPR40-expressing CHO-K1 cells were plated overnight in 384-well plates (4,000 cells per well) in complete media, with or without 100 ng/mL Pertussis Toxin (Tocris, Cat # 3097). The following day, the culture media was replaced with assay buffer containing HBSS with calcium and magnesium, 20 mM HEPES and 0.1% Fatty acid free BSA, pH 7.4. Compounds were then added and incubated with cells at 37 °C for 90 min. Analytes were detected according to the manufacturer's protocol (CisBio IPone Tb kit, Cat # 62IPAPEC). Data presented are representative of at least three independent experiments performed in quadruplicate for each compound. Data are represented as averages  $\pm$  S.D.

### *Calcium measurements*

The day before the assay, hGPR40-expressing CHO-K1 cells were plated overnight in 384-well plates (20,000 cells per well) in complete media. The following day, the culture media was replaced with 25  $\mu\text{L}$  of assay buffer containing HBSS with calcium and magnesium, 20 mM

HEPES and 0.1% Fatty acid free BSA, pH 7.4, and starved for 1 h at 37 °C. Calcium-sensitive fluorescent dye (Fluo 6, Molecular Devices, Cat # R8190) was then added in 25  $\mu$ L assay buffer and the cells incubated for another hour at 37 °C protected from light. Plates were read on the FLIPR Tetra (Molecular Devices) measuring emission at 515-575 nm caused by excitation at 470-495 nm before and up to 8 min after addition of 12.5  $\mu$ L of 5X agonist solution (prepared in assay buffer). The concentration response curves were constructed based on the maximal responses over baseline obtained for different concentrations of each compound. Data presented are representative of three independent experiments performed in quadruplicate for each compound. Data are represented as averages  $\pm$  S.E.M.

#### *cAMP HTRF measurements*

The day before the assay, hGPR40-expressing CHO-K1 cells were plated overnight in 384-well plates (20,000 cells per well) in complete media. The following day, the culture media was replaced with assay buffer containing HBSS with calcium and magnesium, 20 mM HEPES and 0.1% Fatty acid free BSA, pH 7.4, and starved for 1 h at 37 °C. The assay buffer was then replaced with fresh assay buffer containing 500  $\mu$ M IBMX, and compounds were added in assay buffer (no IBMX) for 30 min. Analytes were detected according to the manufacturer's protocol (CisBio cAMP Dynamic kit kit, Cat # 62AM4PEC). Fluorescence was read with a PHERAstar plate reader using an excitation of 337 nm and emissions of 620 and 665 nm. Raw data were converted to nM cAMP by interpolation from a cAMP standard curve.  $E_{max}$  and  $EC_{50}$  determinations were made from an agonist-response curve analyzed with a curve fitting program using a 4-parameter logistic dose response equation in Graphpad Prism 7.0. Data presented are representative of three



independent experiments performed in quadruplicate for each compound. Data are represented as averages  $\pm$  S.D.

#### *DiscoverX arrestin recruitment*

The ability of hGPR40 to recruit  $\beta$ -arrestin-2 was determined using the DiscoverX PathHunter technology (DiscoverX) that involves enzyme complementation of fusion-tagged receptor along with an arrestin recruitment modulating sequence and  $\beta$ -arrestin-2 proteins. DLD1 cells expressing hGPR40 (DiscoverX) were seeded in Cell Plating Media 2 (DiscoverX, Cat # 93-0563R2A) at a density of 15,000 cells/well in 384-well black, clear-bottom plates. The following day, the culture media was replaced with assay buffer containing HBSS with calcium and magnesium, 20 mM HEPES and 0.1% Fatty acid free BSA, pH 7.4, and starved for 1 h at 37 °C. The cells were then treated with multiple concentrations of agonists in PBS and incubated at 37 °C for 60 minutes. DiscoverX reagent was then added to the cells according to the manufacturer's recommendations followed by 1 h incubation at room temperature and luminescence was measured on a PHERAstar reader. Data presented are representative of three independent experiments performed in triplicate for each compound. Data are represented as averages  $\pm$  S.D.

#### *Bioluminescence resonance energy transfer (BRET)-based biosensor assays (BioSensAll®)*

BioSensAll® biosensor assays were conducted at Domain Therapeutics NA Inc. (Montreal, QC, Canada). Assays were performed in HEK-293T cells, cultured in Dulbecco's Modified Eagle Medium (DMEM) (Wisent, Cat # 319-015-CL) supplemented with 1% penicillin-streptomycin (Wisent, Cat # 450-201-EL) and 10% fetal bovine serum (Wisent, Cat # 090150) and maintained at 37 °C with 5% CO<sub>2</sub>. All biosensor-coding plasmids and related information are the property of

Domain Therapeutics NA Inc.: GAPL-Gs (Cat # DTNA A27), GAPL-Gq (Cat # DTNA A34), GAPL-G11 (Cat # DTNA A35), GAPL-Gi2 (Cat # DTNA A29), GAPL-GoB (Cat # DTNA A32), GAPL-Gz (Cat # DTNA A33) and GAPL-G12 (Cat # DTNA A38). Transfections were performed using 25-kDa linear PEI (Polysciences, Warrington, PA) at a 3:1  $\mu\text{L}$  of PEI/ $\mu\text{g}$  of DNA ratio. Briefly, DNA and PEI were diluted separately in 150 mM NaCl, mixed and then incubated for at least 20 minutes at room temperature (note: total amount of DNA transfected was adjusted to a final quantity of 2  $\mu\text{g}$  with salmon sperm DNA (Invitrogen)). During the 20-minute incubation, HEK-293T cells were detached, counted and re-suspended into cell culture medium to a final density of 350,000 cells/mL. At the end of the 20-minute incubation, DNA/PEI complexes were added to the cells followed by gentle mixing. Cells were subsequently distributed in cell culture-treated 96-well plates (White Opaque 96-well Microplates, Greiner, Cat # 655) at a density of 35,000 cells per well (i.e., 100  $\mu\text{L}$  of cell suspension per well) and incubated at 37 °C for 48 h. For PTX treatment, 24 hours after transfection and the day before the assay, the medium was replaced by fresh medium containing 100 ng/mL Pertussis Toxin (Tocris, Cat # 3097). 48 hours after the transfection, the transfection medium was removed and cells were washed once with 100  $\mu\text{L}$  of Tyrode-HEPES buffer (Sigma, Cat # T2145-H9136) per well. Wash buffer was then replaced with 100  $\mu\text{L}$  of fresh Tyrode-HEPES buffer per well and plates were incubated for 60 min at room temperature. At the end of this equilibration period, 10  $\mu\text{L}$  of 20  $\mu\text{M}$  e-Coelenterazine Prolume Purple (Methoxy e-CTZ; Nanolight, Cat # 369) was added to each well followed immediately by the addition of increasing test compound concentrations. For PAM mode experiments, 10 minutes after the addition of increasing concentrations of test compound, an EC20 of  $\alpha$ -linolenic acid (1  $\mu\text{M}$ ) was added to the cells. Cells were incubated at room temperature for 10 minutes and BRET readings subsequently collected with a 0.4 sec integration time on a Synergy NEO plate reader

(BioTek Instruments, Inc., USA; filters: 400nm/70nm and 515nm/20nm, donor and acceptor filters respectively). The BRET signal was calculated as the ratio of acceptor emission to donor emission. Data from at least three independent experiments for each compound and performed in duplicates were combined and symbols presented are the mean  $\pm$  S.E.M.

Note that due to the nature of the sensors, apart from the GAPL-Gs sensor whose activation leads to a decrease in the BRET signal, activation of the other sensors leads to an increase in the BRET signal.

To calculate the bias factor between some of those pathways for our compounds, we used the Black–Leff operational model to fit the agonist concentration ( $[A]$ )–response curves as follows (Kenakin *et al.*, 2012):

$$\text{response} = \frac{E_m[A]^n\tau^n}{[A]^n\tau^n + ([A] + K_A)^n}$$

where the maximal response of the system is given by  $E_m$ , while  $n$  is the “transducer slope” for the function linking agonist concentration to measured response and the parameters  $K_A$  and  $\tau$  as the equilibrium constants governing the “reaction”.  $\text{Log}(\tau/K_A)$  is defined as the transduction coefficient and using  $\alpha$ -linolenic acid as a reference, we calculated the relative efficiency of our compounds at relevant pathways  $[\Delta\log(\tau/K_A)]$ . The bias factor  $[\Delta\Delta\log(\tau/K_A)$  or log bias] between pathways  $j_1$  and  $j_2$  can be calculated as follows:

$$\text{bias} = 10^{\Delta\Delta\log(\tau/K_A)_{j_1-j_2}}$$

where

$$\Delta\Delta\log(\tau/K_A)_{j_1-j_2} = \log \text{bias} = \Delta\log(\tau/K_A)_{j_1} - \Delta\log(\tau/K_A)_{j_2}$$

### *Molecular modeling*

Molecular modeling and docking has been performed using the recent co-crystal structure of hGPR40 in complex with MK-8666 and AgoPAM AP8 (PDB code 5TZY) (Lu *et al.*, 2017). MOE (Molecular Operating Environment, 2015.1001, Chemical Computing Group Inc., 1010 Sherbooke St. West, Suite #910, Montreal, QC, Canada) was used for loop modeling, energy minimization (AMBER10:EHT forcefield and Born solvation model) and rescoring of the docking poses. Glide was used for molecular docking of Compound A (Small-Molecule Drug Discovery Suite 2016-3: Glide, version 6.9, Schrödinger, LLC). The docking poses generated with Glide-XP were rescored using the GBVI/WSA dG scoring function available in MOE (Corbeil *et al.*, 2012). The top ranked pose of Compound A was imported, with the hGPR40 protein structure, into a Pymol session to create all pictures (The PyMOL Molecular Graphics System, Version 1.8 Schrödinger, LLC).

### *Radioligand binding experiment*

Membranes were prepared as follows. Cells stably expressing hGPR40 were harvested by centrifugation (10 min at 5,000 g). The pellet was resuspended in lysis buffer [10 mM Tris-HCl, pH 7.4, 137 mM NaCl, and Complete protease inhibitor cocktail (Roche, Cat # 11873580001: 1 tablet per 40 mL)], and lysed using 30 strokes with a Dounce homogenizer on ice. The homogenate was centrifuged at 4 °C (10 min at 900 g). The supernatant was centrifuged at 4 °C for 60 min at 100,000 g. The resulting pellet was resuspended in wash buffer [10 mM Tris-HCl, pH 7.4, 1 M NaCl, and Complete protease inhibitor cocktail (1 tablet per 40 mL)]. The homogenate was

centrifuged at 4 °C for 30 min at 100,000 g. Membranes were resuspended at 10 mg/mL protein in 10 mM Tris-HCl, pH 7.4, and 137 mM NaCl.

Test compounds were serially diluted in binding buffer (PBS + 0.1% fatty acid-free BSA). Each well of the 96-well assay plate contained diluted test compounds, 50 nM [<sup>3</sup>H]-Compound A or 10 nM [<sup>3</sup>H]-AM-1638, and 10 µg/well hGPR40 membrane suspension in a total volume of 100 µL. The binding reaction was allowed to equilibrate for 60 minutes at room temperature with shaking. Binding assays were terminated using a Harvester Filtermate 96 (PerkinElmer). Bound and free radioligands were separated by collecting the membrane-bound fraction onto GF/B filterplates impregnated with PEI 0.5% and pre-wetted with binding buffer. Filterplates were washed 4 times with ice-cold binding buffer and dried for 2 hours. Microscint O (50 µL) was added to each well and radioactivity was counted using the Topcount (PerkinElmer). Nonspecific binding was determined using 10 µM cold Compound A or AM-1638. Data analysis was performed using GraphPad Prism 7.0 (GraphPad Software, Inc., La Jolla, CA, 92037, USA). Data presented are representative of three independent experiments performed in triplicate for each compound. Data are represented as averages ± S.D.

For receptor densities evaluation, whole cell saturation binding experiments were performed according to what has been previously described (Jin *et al.*, 2009), using a binding buffer composed of DMEM, 25 mM HEPES and 0.1 % fatty acid-free BSA (pH 7.4). For receptor number determination, a normalization sample (Norm) was used and the receptor density was calculated as follows:

$$\text{Number of receptors per cell} = \frac{6.022 \cdot 10^{23} \cdot B_{\max} \cdot \text{number of mol radioligand used for NORM}}{\text{Number of cells} \cdot \text{CPM of NORM}}$$

*Insulin secretion in human islets*

Human islets were dispersed with Accutase (Thermo Fisher Scientific, Cat # A1110501) for 10 minutes at 37 °C. 20,000 cells per well were plated in V-bottom 96-well plates and cultured overnight in complete medium containing: CMRL Media (Thermo Fisher Scientific, Cat # 11530-037), 10 mM Niacinamide, [1 mg/mL, 0.55 mg/mL, 0.67 ug/mL] ITS (Thermo Fisher Scientific, Cat # 41400045), 16.7 mM Zinc Sulfate, 5 mM Sodium Pyruvate, 2 mM Glutamax (Thermo Fisher Scientific, Cat # 35050-061), 25 mM HEPES and 10% FBS. The next day, medium was replaced with assay buffer (Krebs Ringer) and cells were pre-incubated in 2 mM glucose for 1 hour. Next, the indicated concentrations of compounds were added in either 2 mM or 12 mM glucose and the cells were incubated at 37 °C for 1 hour. The supernatant was then collected and tested for insulin using the CioBio HTRF Insulin assay kit (Cat # 62INSPEC). Data are represented as averages  $\pm$  S.E.M. from 3 different islets. Donors are different between graphs A and B. Statistical significance was determined by one-way ANOVA with Dunnett post hoc analysis using GraphPad Prism 7.0 (GraphPad Software, Inc., La Jolla, CA, 92037, USA).

### *Statistics*

All data are expressed as the mean  $\pm$  SEM or SD as indicated in the Methods and Figures' legends of the indicated number of experiments. Statistical significance was determined by one-way ANOVA with Dunnett post hoc analysis using GraphPad Prism 7.0 (GraphPad Software, Inc., La Jolla, CA, 92037, USA).

### *Materials*

The synthesis of Compound A is summarized in the Supplemental Methods. Forskolin and IBMX were obtained from Tocris Bioscience (Bristol, UK). DMEM/F12 (Cat # 11320033) and

DMEM/High Glucose media (Cat # 11965175), penicillin/streptomycin (Cat # 15140122), L-Glutamine (Cat # 25030081), G418 (Cat # 10131027) and Hygromycin (Cat # 10687010) were purchased from Thermo Fisher Scientific (MA, USA). FBS (Hyclone Cat # SH30070.03) was purchased from GE Healthcare (IL, USA). HBSS (Cat # 21-023-CV) and HEPES (Cat # 25-060-CI) were purchased from CellGro (VA, USA). Fatty acid free BSA (Cat # A9205) was purchased from Sigma-Aldrich (St. Louis, MO, USA). Human islets were obtained from healthy donors through Prodo (Prodo Laboratories Inc, CA, USA, 92656).

## Results

### Identification and characterization of a new hGPR40 full agonist

#### *Compound A is a full agonist at the IP1/calcium pathway*

Multiple series of hGPR40 agonists were rationally designed based on existing structures and evaluated in a calcium assay using a hGPR40 low-expressing CHO-K1 stable cell line to allow differentiation between partial and full agonists. In this assay, Compound A (Figure 1A; Supplemental Methods) showed similar efficacy to AM-1638, previously reported as a highly efficacious hGPR40 full agonist (Hauge *et al.*, 2015; Li *et al.*, 2016), while fasiglifam was only weakly efficacious (Figure 1B). To confirm the activity of Compound A, we used an IP1 HTRF® assay that detects the accumulation of IP1 inside the cells that follows the rapid degradation of IP3 (Figure 1C). The IP1 HTRF® assay has indeed been shown to generate less false positive results (Cassutt *et al.*, 2007). Compound A was as efficacious as AM-1638 and showed superior efficacy compared to fasiglifam ( $E_{\max}$  fasiglifam =  $50.9 \pm 1.2\%$  compared to that of Compound A\*\*\*\*,  $p < 0.0001$ ) (Figure 1C). However, compared to Compound A and AM-1638 ( $EC_{50} = 225 \pm 80$  nM and  $158 \pm 27$  nM respectively) (Figure 1C), fasiglifam ( $EC_{50} = 78 \pm 30$  nM) was about 2-3 times more potent (\*,  $p < 0.05$ ).

We also profiled the activity of Compound A at the  $\beta$ -arrestin2 pathway and obtained similar results (Supplemental Figure 1), with fasiglifam inducing about 50% efficacy compared to the full agonists ( $51.2 \pm 8.3\%$ \*\*\*\*,  $p < 0.0001$ ). No significant bias was observed for any of the compounds between  $G\alpha q/11$  and  $\beta$ -arrestin2.

#### *Compound A is fully efficacious at potentiating GSIS in human islets*



We then tested the ability of Compound A to potentiate GSIS in human islets from healthy donors. All donors tested were responsive to 12 mM glucose and non-glucose dependent insulin secretagogues, KCl and Glibenclamide. In the presence of 12 mM glucose, Compound A (3 and 10  $\mu$ M) significantly potentiated insulin secretion ( $79.6 \pm 18.5$  ng/mL and  $78.7 \pm 10.2$  ng/mL, respectively;  $p < 0.0001$ ) compared to islets treated with glucose alone ( $11.6 \pm 6.2$  ng/mL) (Figure 2A). Fasiglifam potentiated 12 mM glucose-induced insulin secretion ( $26.7 \pm 15.9$  ng/ml,  $p = 0.0008$ ) but to a lesser extent than Compound A ( $22.4 \pm 6\%$  of the potentiation induced by Compound A,  $p < 0.0001$ ). The effects observed with Compound A and fasiglifam were consistent with the potentiation induced by AM-1638 compared to other partial agonists (Luo *et al.*, 2012). Interestingly, in the presence of 2 mM glucose, whereas Compound A (3 and 10  $\mu$ M) significantly potentiated insulin secretion ( $16.6 \pm 4.7$  ng/mL and  $41.2 \pm 12.1$  ng/mL, respectively;  $p < 0.0001$ ) compared to islets treated with glucose alone ( $3.9 \pm 1.2$  ng/mL) (Figure 2B), fasiglifam was inactive.

### **Compound A is an allosteric full agonist at $G\alpha_q$ , $G\alpha_i2$ and $G\alpha_{12}$**

*Compound A is a full agonist at  $G\alpha_q$  and  $G\alpha_i2$ , and engages the  $G\alpha_{12}$  pathway*

In addition to the  $G\alpha_q$ /IP1/calcium pathway, some GPR40 agonists have been shown to activate alternative pathways (Mancini *et al.*, 2015; Schroder *et al.*, 2011) (Defossa *et al.*, 2014; Hauge *et al.*, 2015; Lin *et al.*, 2012). Thus, we used BRET (Bioluminescence Resonance Energy Transfer)-based biosensors to fully characterize other G-proteins downstream of hGPR40 activation. Resonance energy transfer between a luminescent enzymatic donor and a fluorescent protein acceptor typically occurs in the 1-10 nm range, which makes BRET an ideal platform to study protein-protein interactions in living cells. BRET has indeed been extensively used to study G

proteins activation by multiple GPCRs (Denis *et al.*, 2012; Namkung *et al.*, 2016; Salahpour *et al.*, 2012) and allows monitoring in real time the activation of G proteins of interest following GPR40 agonist treatment. We first used  $G\alpha_q$ - and  $G\alpha_{11}$ -sensors (Figure 3A and Supplemental Figure 2A) to confirm the engagement of those pathways. IP1 production can indeed originate from other G protein couplings (Rives *et al.*, 2009) and BRET sensors provide a straightforward approach to directly assess G protein activation, independently of downstream effectors and potential cross regulation between pathways. Compared to the IP1 assay, we obtained similar results with the  $G\alpha_q$ - and  $G\alpha_{11}$ -sensors (Figure 3A and Supplemental Figure 2A). Compound A was a full agonist at the  $G\alpha_q$  and  $G\alpha_{11}$  pathways with similar efficacy as  $\alpha$ -linolenic acid, an endogenous GPR40 agonist, as well as AM-1638 and fasiglifam was a partial agonist with about 40% efficacy (Table 1; Figure 3A;  $p < 0.0001$ ). However, in contrast to the IP1 assay, fasiglifam was less potent than Compound A and AM-1638 at recruiting  $G\alpha_q$  (Table 1), suggesting fasiglifam might trigger the activation of other pathways leading to IP1 accumulation. Additionally, at both the  $G\alpha_q$  and  $G\alpha_{11}$  pathways, Compound A- and AM-1638-induced responses, but not that induced by fasiglifam, appeared highly cooperative (Hill Slope  $> 1$ ) (Table 1).

We then measured the ability of Compound A to activate the  $G\alpha_i/o$  pathway in hGPR40 expressing cells using  $G\alpha_{i2}$  (Figure 3B),  $G\alpha_oB$  and  $G\alpha_z$  sensors (Table 1). Both Compound A and AM-1638 were full agonists at the  $G\alpha_i/o$  pathway (Figure 3B; Table 1) compared to  $\alpha$ -linolenic acid, with Compound A being slightly more potent (Table 1). Interestingly, fasiglifam displayed intra-  $G\alpha_i/o$  family bias by promoting partial activation of  $G\alpha_{i2}$  (~50% efficacy compared to Compound A and AM-1638) while being completely inactive on  $G\alpha_oB$  and  $G\alpha_z$  (Figure 3B; Table 1).

Compared to Compound A and AM-1638, fasiglifam was more potent at recruiting  $G\alpha i2$  than  $G\alpha q/11$  (Figure 3A and B; Table 1). Using the Black–Leff operational model and  $\alpha$ -linolenic acid as a reference compound, we evaluated that fasiglifam was biased toward  $G\alpha i2$  vs.  $G\alpha q$  (Bias factor = 5.86 compared to 0.19 for both Compound A and AM-1638) while Compound A and AM-1638 were slightly biased towards  $G\alpha q$  vs  $G\alpha i2$  (Bias factor = 5.2 compared to 0.17 for fasiglifam). These data could explain why fasiglifam was more potent than Compound A and AM-1638 at the IP1 pathway compared to the  $G\alpha q$  activation assay. It is in fact well known that  $G\alpha i/o$  coupling can lead to IP production and calcium signaling (Rives *et al.*, 2009). To confirm the involvement of the  $G\alpha i/o$  pathway in fasiglifam-induced IP1 responses, we measured GPR40-mediated IP1 production following treatment with Compound A, AM-1638 and fasiglifam in presence of Pertussis Toxin (PTX). PTX activity was first validated using the BRET  $G\alpha q$  and  $G\alpha i2$  sensors. While PTX had no significant effect on  $G\alpha q$  activation (Supplemental Figure 3A), it completely abolished  $G\alpha i2$  coupling (Supplemental Figure 3B). The efficacy of Compound A and AM-1638 at inducing IP1 production was not significantly affected by PTX treatment but the potency of both compounds was slightly reduced ( $3.5 \pm 0.4$ -fold and  $2.4 \pm 0.1$ -fold, respectively) (Supplemental Figures 3C and 3D). However, fasiglifam-induced IP1 response was almost completely abolished by PTX treatment (Supplemental Figure 3E), suggesting that in contrast to Compound A and AM-1638, fasiglifam-induced IP1 production was mostly driven by  $G\alpha i/o$  coupling.

We also profiled the activity of Compound A at the  $G\alpha 12/13$  pathway. Interestingly, while fasiglifam failed to recruit  $G\alpha 12$ , Compound A and AM-1638 strongly activated the  $G\alpha 12$  protein in hGPR40 expressing cells (Figure 3C; Table 1). The magnitude of the  $G\alpha 12$  response following

activation of hGPR40 by Compound A and AM-1638 was substantial and similar to that induced by ghrelin in cells expressing the ghrelin receptor (Supplemental Figure 2B) (Evron *et al.*, 2014; Sivertsen *et al.*, 2011). Interestingly,  $\alpha$ -linolenic acid only very weakly activated the pathway, suggesting that the ability to activate G $\alpha$ 12 is a unique property of the synthetic full agonists AM-1638 and Compound A. We obtained similar results at G $\alpha$ 13 (Supplemental Figure 2C). Although the G $\alpha$ 12/G13-mediated signaling pathway is poorly understood, it has been linked to protein kinase D (PKD) activation as well as actin remodeling (Siehler, 2007; Yuan *et al.*, 2001), which are well known to contribute to the release of vesicles.

#### *Compound A only weakly triggers G $\alpha$ s activation/cAMP production*

As mentioned previously, it has been shown that in addition to the G $\alpha$ q/IP1/calcium pathway, some GPR40 agonists could induce coupling to other pathways (Hauge *et al.*, 2017; Hauge *et al.*, 2015; Mancini *et al.*, 2015; Mancini *et al.*, 2013; Schroder *et al.*, 2011). More specifically, it has been shown that allosteric full agonists such as AM-1638, but not partial agonists, induced coupling to the G $\alpha$ s/cAMP pathway and that only agonists at both G $\alpha$ q and G $\alpha$ s could trigger maximal efficacy in relevant preclinical models, such as GLP-1 secretion in mice (Hauge *et al.*, 2015; Luo *et al.*, 2012). To assess the ability of Compound A to induce signaling through the G $\alpha$ s/cAMP pathway, we also used a BRET-based G $\alpha$ s sensor (Figure 4A). In cells transfected with the glucagon-like peptide 1 (GLP-1) receptor, a well-known G $\alpha$ s-coupled receptor, GLP-1[7-36] induced a strong G $\alpha$ s response, confirming the functionality of the G $\alpha$ s biosensor. However, in hGPR40-transfected cells, only a very weak response could be measured after stimulation with either Compound A or  $\alpha$ -linolenic acid, about 10-20% of the GLP-1 response. Fasiglifam was

inactive (Figure 4A). Surprisingly, AM-1638 also only weakly induced G $\alpha$ s activation (Figure 4A).

To confirm those findings, we also measured cAMP accumulation in the hGPR40 stable CHO-K1 cell line mentioned previously. As previously described (Hauge *et al.*, 2015), fasiglifam was inactive and did not induce any significant increases in cAMP accumulation. Interestingly, although Compound A and AM-1638 induced some cAMP accumulation, the magnitude of the cAMP response was very weak compared to the forskolin control performed in the same cells (Figure 4B).

#### *Compound A is an allosteric full agonist*

Three distinct binding sites have been described for GPR40, one which binds endogenous fatty acids such as  $\alpha$ -linolenic acid, one which binds partial agonists such as fasiglifam and one which binds allosteric full agonists, such as AM-1638 and the recently reported AP8 (Defossa *et al.*, 2014; Hauge *et al.*, 2015; Lin *et al.*, 2012; Lu *et al.*, 2017; Srivastava *et al.*, 2014). The resolution of the crystal structure of the human GPR40 in complex with both a partial agonist and the full agonist AP8, recently identified the allosteric full agonists' binding site as a lipid-facing pocket outside the transmembrane helical bundle (Lu *et al.*, 2017), between TM4 and TM5.

To assess the orthosteric or allosteric nature of Compound A, we analyzed the functional cooperativity between  $\alpha$ -linolenic acid and Compound A using BRET-based G $\alpha$ q (Figure 5A) and G $\alpha$ i2 sensors (Figure 5B), compared to that of fasiglifam and AM-1638. All three compounds could potentiate an EC<sub>20</sub> of  $\alpha$ -linolenic acid at inducing G $\alpha$ q and G $\alpha$ i2 coupling. The relative potencies and efficacies of Compound A, AM-1638 and fasiglifam in PAM (positive allosteric

modulator) mode (Figure 5) were consistent with those previously observed in agonist mode (Figure 3). Compound A ( $0.17 \pm 0.04$  nM and  $2.0 \pm 0.4$  nM at  $G\alpha_q$  and  $G\alpha_i2$ , respectively) was slightly more potent than AM-1638 ( $0.6 \pm 0.3$  nM and  $5.0 \pm 1.5$  nM at  $G\alpha_q$  and  $G\alpha_i2$ , respectively) at potentiating  $\alpha$ -linolenic acid-induced  $G\alpha_q$  and  $G\alpha_i2$  coupling. Moreover, compared to Compound A and AM-1638, fasiglifam only induced a partial potentiation of  $\alpha$ -linolenic acid responses ( $60 \pm 6$  % and  $53 \pm 3$  % at  $G\alpha_q$  and  $G\alpha_i2$ , respectively; Figure 5). Those data confirm the allosteric nature of Compound A, potentiating  $\alpha$ -linolenic acid-induced responses.

We then used a computational approach to assess whether Compound A could bind to the same binding site as other reported allosteric full agonists. Compound A was docked in the lipid-facing pocket identified by Lu and colleagues between TM4 and TM5. The best docking pose of Compound A revealed a similar binding mode as AP8 (Figure 6A). Among the interactions between Compound A and the protein, the carboxylate group anchored the compound between TM4 and TM5 via a complex H-bond network with Ser123, Tyr44 and probably with Tyr114 from Intracellular Loop 2, folded in an alpha helix in presence of the full agonists (Figure 6B). The 5-fluoro-2-methoxy phenyl ring formed a CH... $\pi$  interactions with the side chain of Pro194. The rest of the Compound A made numerous Van der Waals contacts with the hydrophobic residues forming the binding grove (Ala98, Ala99, Ala102, Val126, Ile130, Leu193 and Ile197) (Figure 6B). While it is clear that multiple ligand: protein interactions contribute to the potency of the Compound A, the physicochemical properties of the compound suggests it could also make numerous contacts with surrounding membrane lipids (missing in the x-ray structure).

Furthermore, we also performed radioligand binding experiments using both [ $^3$ H]-Compound A and [ $^3$ H]-AM-1638, providing additional evidence that Compound A could bind to the same site as AM-1638. Competition binding experiments showed that Compound A, as well as AM-1638

completely displaced the binding of both [<sup>3</sup>H]-Compound A (Supplemental Figure 4A) and [<sup>3</sup>H]-AM-1638 (Supplemental Figure 4B). Data were fitted quite well by a one-site competition binding model (Supplemental Table 1), providing additional evidence that both compounds bind to an identical unique binding site. Additionally, fasiglifam had a positive cooperative effect on the binding of [<sup>3</sup>H]-Compound A (Supplemental Figure 4A). The effects observed with fasiglifam are similar to those previously reported in the literature (Lu *et al.*, 2017; Plummer *et al.*, 2017; Yabuki *et al.*, 2013) and are consistent with the allosteric nature of this compound.

## **Discussion**

GPR40 is a clinically validated molecular target for the treatment of diabetes. Although the partial agonist fasiglifam (TAK-875) showed efficacy in phase III clinical trials, its efficacy did not significantly differentiate from glimepiride and attention has shifted toward the development of full agonists that exhibit superior efficacy in preclinical models (Hauge *et al.*, 2017; Hauge *et al.*, 2015; Luo *et al.*, 2012; Mancini *et al.*, 2015; Schroder *et al.*, 2011). In the present study, we described the pharmacology of Compound A, a newly identified GPR40 allosteric full agonist at the  $G\alpha_q$ /IP1/calcium pathway fully efficacious at enhancing GSIS in human islets. We compared Compound A-induced GPR40 activity at a panel of G proteins and to that of both fasiglifam and AM-1638, another allosteric full agonist previously reported to be highly efficacious in preclinical models (Hauge *et al.*, 2015; Luo *et al.*, 2012).

In human islets, in presence of high glucose, Compound A was highly efficacious at potentiating insulin secretion and data were consistent with those reported for AM-1638 (Luo *et al.*, 2012). Despite 40-50% efficacy compared to Compound A and AM-1638 at the  $G\alpha_q$ /IP1/calcium pathway, in human islets and in presence of high glucose, fasiglifam efficacy was only about 22.4% of that of Compound A at potentiating insulin secretion. Moreover, Compound A, but not fasiglifam, could potentiate insulin secretion in low glucose conditions. These data suggest that the pharmacology of GPR40 is complex and that the activation of additional pathways might be responsible for the superior efficacy of Compound A in human islets.

Previous studies have suggested that activation of alternative pathways in addition to the  $G\alpha_q$ /calcium pathway was required for maximal efficacy in preclinical models (Defossa *et al.*,



2014; Hauge *et al.*, 2015; Lin *et al.*, 2012). Thus, only allosteric full agonists, such as AM-1638, that in addition to the  $G\alpha_q$ /calcium pathway were shown to induce cAMP production, could trigger maximal efficacy in preclinical models, such as GLP-1 secretion in mice (Hauge *et al.*, 2017; Hauge *et al.*, 2015; Luo *et al.*, 2012). Interestingly, even though Compound A binds to the same site as AM-1638 (Figure 6; Supplemental Figure 4), it showed no to very little efficacy at the  $G\alpha_s$ /cAMP pathway. The magnitude of the cAMP response produced after stimulation with Compound A was very low and hGPR40 only very weakly coupled to  $G\alpha_s$  after stimulation with Compound A (Figure 4). Surprisingly, AM-1638 also only weakly induced  $G\alpha_s$  activation and it is noteworthy that the magnitude of cAMP accumulation observed was similar to that previously reported (Hauge *et al.*, 2015). Thus, although we cannot exclude the possibility that weak GPR40-mediated cAMP accumulation is enough to potentiate GLP-1 secretion or that mouse GPR40 coupling properties might significantly differ from human GPR40, our data suggest that hGPR40 does not efficiently couple to the  $G\alpha_s$ /cAMP pathway and that pathways other than  $G\alpha_s$  might be involved in GPR40 agonists *in vivo* efficacy. Moreover, our findings suggest that cAMP production measured *in vitro* may originate from other non- $G\alpha_s$  mediated couplings. It has indeed been shown that some adenylyl cyclase isoforms are calcium-sensitive (Halls *et al.*, 2011) raising the possibility that the weak cAMP responses observed after GPR40 stimulation could come from cross regulation between pathways.

We therefore assessed the ability of our compound to induce the activation of other G proteins. Figure 7 shows an efficacy plot representing the relative efficacy of Compound A and AM-1638 as well as fasiglifam, relative to  $\alpha$ -linolenic acid at multiple G proteins. The graph highlights the ability of Compound A and AM-1638 to activate the  $G\alpha_q/11$  and  $G\alpha_i/o$  protein families, while fasiglifam was only a partial agonist at some of those pathways. The poor efficacy of fasiglifam is

consistent with recent crystallography studies, showing that in complex with fasiglifam, the intracellular portion of the receptors was in an “inactive-like” state (Lu *et al.*, 2017; Srivastava *et al.*, 2014). Moreover, in contrast to fasiglifam, at both  $G\alpha_q$  and  $G\alpha_{11}$ , Compound A- and AM-1638-induced responses appeared highly cooperative (Hill Slope > 1) (Table 1). Since the binding data (Figure 6, Supplemental Figure 4 and Supplemental Table 1) suggest the existence of only one binding site for those compounds, it is likely that Compound A and AM-1638 stabilize a unique conformation of the receptor, distinct from that stabilized by fasiglifam and that this conformation is further stabilized by  $G\alpha_q$ , but not other G proteins. It is indeed now well known that downstream effectors such as G proteins can allosterically modulate the receptor and stabilize active or inactive conformations (Rasmussen *et al.*, 2011).

Although activation of the  $G\alpha_q$ /IP1/ $Ca^{2+}$  pathway was shown to lead to insulin secretion and  $G\alpha_i/o$  coupling is known to potentiate  $G\alpha_q$ -mediated IP1 and calcium responses (Rives *et al.*, 2009), the activation of  $G\alpha_i/o$ -coupled receptors is usually associated with a decrease in GSIS, through the inhibition of adenylyl cyclases (Fridlyand *et al.*, 2016). In contrast to Compound A and AM-1638, fasiglifam appeared slightly biased toward  $G\alpha_i2$  vs  $G\alpha_q$  and fasiglifam-induced IP1 production was more sensitive to PTX treatment than that of Compound A and AM-1638. The extent to which these differences contribute to differences in efficacy and/or safety is not clear but it could explain the weak efficacy of fasiglifam at potentiating GSIS (< 25%) despite 40-50% efficacy compared to Compound A and AM-1638 at the  $G\alpha_q$ /IP1 pathway.

Compound A and AM-1638 also induced hGPR40 coupling to  $G\alpha_{12}$  (Figure 3C), while fasiglifam was inactive and  $\alpha$ -linolenic acid only weakly activated the pathway. Although other agonists

should be evaluated in this assay, those data suggest that the ability to activate  $G\alpha_{12}$  is a unique property of synthetic allosteric full agonists. The role of the  $G\alpha_{12}/13$  pathway in insulin and incretin secretion is poorly understood but it has been linked to protein kinase D (PKD) activation as well as actin remodeling, well known to contribute to vesicles release (Arous *et al.*, 2015; Ferdaoussi *et al.*, 2012; Kalwat *et al.*, 2013; Siehler, 2007). Insulin secretion in response to glucose is biphasic, with a rapid and transient first phase followed by a slower but prolonged second phase. It is believed that first-phase insulin secretion corresponds to the exocytosis of a readily-releasable pool of insulin granules pre-docked at the plasma membrane, whereas the second phase relies on the mobilization of an intracellular granule pool to the plasma membrane via a process that requires cytoskeletal remodeling. PKD activation has also been linked to the second-phase of insulin release (Ferdaoussi *et al.*, 2012; Kalwat *et al.*, 2013).

The  $G\alpha_{12}/G_{13}$  proteins activate the monomeric GTPases RhoA. RhoA effectors include Rho kinase (ROCK) which leads to Jun kinase activation and the induction of actin stress fiber formation (Siehler, 2007). The involvement of the cytoskeleton in secretion mechanisms was proposed almost 50 years ago and although the precise mechanisms are not yet fully understood, it is now well accepted that actin regulates insulin granule trafficking and exocytosis (Arous *et al.*, 2015). Constitutively active  $G\alpha_{12}/13$  were found to induce stress fiber formation and focal adhesion assembly in fibroblasts, similarly to activated  $G\alpha_{12}/13$ -linked lysophosphatidic acid receptors and constitutively active RhoA<sup>Q63L</sup> (Siehler, 2007). This suggests that  $G\alpha_{12}$  activation might play a critical role in secretion mechanisms and our data raise the intriguing possibility that despite weak  $G\alpha_s$  signaling, the ability of Compound A and AM-1638 to signal through the  $G\alpha_{12}$  pathway may contribute to the release of vesicles and be an important determinant of GPR40 agonist efficacy. It would be interesting to assess the efficacy of Compound A in mice at inducing GLP-1 secretion,

as well as in T2D human islets, where actin remodeling has been shown to be altered (Arous *et al.*, 2015). Although the role of G $\alpha$ 12/13 downstream of GPR40 in insulin and incretin secretion needs to be validated both *ex vivo* and *in vivo*, while Compound A was more potent at G $\alpha$ q and G $\alpha$ i2 compared to G $\alpha$ 12 (Table 1), in human islets, it is noteworthy that Compound A showed maximal efficacy only at concentrations greater than 1  $\mu$ M (Figure 2).

Nevertheless, the superior efficacy of Compound A in human islets in low glucose conditions, suggests that Compound A administration might lead to hypoglycemia and activation of G $\alpha$ 12/13 could be contra-indicated to avoid insulin secretion in low glucose conditions. Moreover, in addition to its role in insulin secretion, PKD activation has been linked to NF- $\kappa$ B activation, the development of inflammation and pancreatitis (Yuan *et al.*, 2016). Although GPR40 does not seem expressed in the exocrine pancreas, it would be interesting to assess whether Compound A could yield inflammatory responses after either acute or chronic treatment.

In conclusion, we have identified Compound A, a new GPR40 allosteric full agonist fully efficacious at enhancing GSIS in human islets. Compound A was a full agonist at G $\alpha$ q, G $\alpha$ i2 and G $\alpha$ 12, with no to very weak efficacy at the G $\alpha$ s/cAMP pathway. Although more work is needed to validate the role of GPR40-mediated G $\alpha$ 12 pathway in secretion mechanisms, our data suggest that the pharmacology of GPR40 is complex and that engagement of multiple signaling pathways may be critical to achieve sufficient therapeutic efficacy.

**Acknowledgments:**

We would like to thank Dr. Alan Wickenden for his helpful comments on the manuscript.

**Authorship contributions:**

Participated in research design: Rives, Bakaj, Zhao, Rady, Lee, Player and Poci

Conducted experiments: Rives, Rady, Swanson, Zhao, Qi, Bakaj and Mancini

Contributed new reagents or analytic tools: Player

Performed data analysis: Rives, Bakaj, Zhao, Arnoult, Rady, Mancini, Breton, Lee, Poci and  
Player

Wrote or contributed to the writing of the manuscript: Rives, Arnoult, Player, Breton, Mancini and  
Rady

## References:

- Arous C, Halban PA (2015). The skeleton in the closet: actin cytoskeletal remodeling in beta-cell function. *American journal of physiology. Endocrinology and metabolism* **309**(7): E611-620.
- Baggio LL, Drucker DJ (2007). Biology of incretins: GLP-1 and GIP. *Gastroenterology* **132**(6): 2131-2157.
- Briscoe CP, Peat AJ, McKeown SC, Corbett DF, Goetz AS, Littleton TR, *et al.* (2006). Pharmacological regulation of insulin secretion in MIN6 cells through the fatty acid receptor GPR40: identification of agonist and antagonist small molecules. *British journal of pharmacology* **148**(5): 619-628.
- Briscoe CP, Tadayyon M, Andrews JL, Benson WG, Chambers JK, Eilert MM, *et al.* (2003). The orphan G protein-coupled receptor GPR40 is activated by medium and long chain fatty acids. *The Journal of biological chemistry* **278**(13): 11303-11311.
- Burant CF, Viswanathan P, Marcinak J, Cao C, Vakilynejad M, Xie B, *et al.* (2012). TAK-875 versus placebo or glimepiride in type 2 diabetes mellitus: a phase 2, randomised, double-blind, placebo-controlled trial. *Lancet* **379**(9824): 1403-1411.
- Cassutt KJ, Orsini MJ, Abousleiman M, Colone D, Tang W (2007). Identifying nonselective hits from a homogeneous calcium assay screen. *Journal of biomolecular screening* **12**(2): 285-287.
- Corbeil CR, Williams CI, Labute P (2012). Variability in docking success rates due to dataset preparation. *Journal of computer-aided molecular design* **26**(6): 775-786.
- Costa-Neto CM, Parreiras ESLT, Bouvier M (2016). A Pluridimensional View of Biased Agonism. *Molecular pharmacology* **90**(5): 587-595.
- Defossa E, Wagner M (2014). Recent developments in the discovery of FFA1 receptor agonists as novel oral treatment for type 2 diabetes mellitus. *Bioorganic & medicinal chemistry letters* **24**(14): 2991-3000.
- Denis C, Sauliere A, Galandrin S, Senard JM, Gales C (2012). Probing heterotrimeric G protein activation: applications to biased ligands. *Current pharmaceutical design* **18**(2): 128-144.
- Edfalk S, Steneberg P, Edlund H (2008). Gpr40 is expressed in enteroendocrine cells and mediates free fatty acid stimulation of incretin secretion. *Diabetes* **57**(9): 2280-2287.
- Evron T, Peterson SM, Urs NM, Bai Y, Rochelle LK, Caron MG, *et al.* (2014). G Protein and beta-arrestin signaling bias at the ghrelin receptor. *The Journal of biological chemistry* **289**(48): 33442-33455.

Ferdaoussi M, Bergeron V, Zarrouki B, Kolic J, Cantley J, Fielitz J, *et al.* (2012). G protein-coupled receptor (GPR)40-dependent potentiation of insulin secretion in mouse islets is mediated by protein kinase D1. *Diabetologia* **55**(10): 2682-2692.

Fridlyand LE, Philipson LH (2016). Pancreatic Beta Cell G-Protein Coupled Receptors and Second Messenger Interactions: A Systems Biology Computational Analysis. *PloS one* **11**(5): e0152869.

Gorski JN, Pachanski MJ, Mane J, Plummer CW, Souza S, Thomas-Fowlkes BS, *et al.* (2017). GPR40 reduces food intake and body weight through GLP-1. *American journal of physiology. Endocrinology and metabolism* **313**(1): E37-E47.

Halls ML, Cooper DM (2011). Regulation by Ca<sup>2+</sup>-signaling pathways of adenylyl cyclases. *Cold Spring Harbor perspectives in biology* **3**(1): a004143.

Hardy S, St-Onge GG, Joly E, Langelier Y, Prentki M (2005). Oleate promotes the proliferation of breast cancer cells via the G protein-coupled receptor GPR40. *The Journal of biological chemistry* **280**(14): 13285-13291.

Hauge M, Ekberg JP, Engelstoft MS, Timshel P, Madsen AN, Schwartz TW (2017). Gq and Gs signaling acting in synergy to control GLP-1 secretion. *Molecular and cellular endocrinology* **449**: 64-73.

Hauge M, Vestmar MA, Husted AS, Ekberg JP, Wright MJ, Di Salvo J, *et al.* (2015). GPR40 (FFAR1) - Combined Gs and Gq signaling in vitro is associated with robust incretin secretagogue action ex vivo and in vivo. *Molecular metabolism* **4**(1): 3-14.

Hedrington MS, Davis SN (2014). Discontinued in 2013: diabetic drugs. *Expert opinion on investigational drugs* **23**(12): 1703-1711.

Holst JJ (2007). The physiology of glucagon-like peptide 1. *Physiological reviews* **87**(4): 1409-1439.

Itoh Y, Kawamata Y, Harada M, Kobayashi M, Fujii R, Fukusumi S, *et al.* (2003). Free fatty acids regulate insulin secretion from pancreatic beta cells through GPR40. *Nature* **422**(6928): 173-176.

Jin J, Mao Y, Thomas D, Kim S, Daniel JL, Kunapuli SP (2009). RhoA downstream of G(q) and G(12/13) pathways regulates protease-activated receptor-mediated dense granule release in platelets. *Biochemical pharmacology* **77**(5): 835-844.

Kaku K, Enya K, Nakaya R, Ohira T, Matsuno R (2015). Efficacy and safety of fasiglifam (TAK-875), a G protein-coupled receptor 40 agonist, in Japanese patients with type 2 diabetes inadequately controlled by diet and exercise: a randomized, double-blind, placebo-controlled, phase III trial. *Diabetes, obesity & metabolism* **17**(7): 675-681.

Kalwat MA, Thurmond DC (2013). Signaling mechanisms of glucose-induced F-actin remodeling in pancreatic islet beta cells. *Experimental & molecular medicine* **45**: e37.

Kenakin T, Christopoulos A (2013). Signalling bias in new drug discovery: detection, quantification and therapeutic impact. *Nature reviews. Drug discovery* **12**(3): 205-216.

Kenakin T, Watson C, Muniz-Medina V, Christopoulos A, Novick S (2012). A simple method for quantifying functional selectivity and agonist bias. *ACS chemical neuroscience* **3**(3): 193-203.

Latour MG, Alquier T, Oseid E, Tremblay C, Jetton TL, Luo J, *et al.* (2007). GPR40 is necessary but not sufficient for fatty acid stimulation of insulin secretion in vivo. *Diabetes* **56**(4): 1087-1094.

Leifke E, Naik H, Wu J, Viswanathan P, Demanno D, Kipnes M, *et al.* (2012). A multiple-ascending-dose study to evaluate safety, pharmacokinetics, and pharmacodynamics of a novel GPR40 agonist, TAK-875, in subjects with type 2 diabetes. *Clinical pharmacology and therapeutics* **92**(1): 29-39.

Li Z, Qiu Q, Geng X, Yang J, Huang W, Qian H (2016). Free fatty acid receptor agonists for the treatment of type 2 diabetes: drugs in preclinical to phase II clinical development. *Expert opinion on investigational drugs* **25**(8): 871-890.

Lin DC, Guo Q, Luo J, Zhang J, Nguyen K, Chen M, *et al.* (2012). Identification and pharmacological characterization of multiple allosteric binding sites on the free fatty acid 1 receptor. *Molecular pharmacology* **82**(5): 843-859.

Lu J, Byrne N, Wang J, Bricogne G, Brown FK, Chobanian HR, *et al.* (2017). Structural basis for the cooperative allosteric activation of the free fatty acid receptor GPR40. *Nature structural & molecular biology*.

Luo J, Swaminath G, Brown SP, Zhang J, Guo Q, Chen M, *et al.* (2012). A potent class of GPR40 full agonists engages the enteroinsular axis to promote glucose control in rodents. *PloS one* **7**(10): e46300.

Mancini AD, Bertrand G, Vivot K, Carpentier E, Tremblay C, Ghislain J, *et al.* (2015). beta-Arrestin Recruitment and Biased Agonism at Free Fatty Acid Receptor 1. *The Journal of biological chemistry* **290**(34): 21131-21140.

Mancini AD, Poitout V (2013). The fatty acid receptor FFA1/GPR40 a decade later: how much do we know? *Trends in endocrinology and metabolism: TEM* **24**(8): 398-407.

Namkung Y, Le Gouill C, Lukashova V, Kobayashi H, Hogue M, Khoury E, *et al.* (2016). Monitoring G protein-coupled receptor and beta-arrestin trafficking in live cells using enhanced bystander BRET. *Nature communications* **7**: 12178.



Otieno MA, Snoeys J, Lam W, Ghosh A, Player MR, Pocai A, *et al.* (2017). Fasiglifam (TAK-875): Mechanistic Investigation and Retrospective Identification of Hazards for Drug Induced Liver Injury. *Toxicological sciences : an official journal of the Society of Toxicology*.

Plummer CW, Clements MJ, Chen H, Rajagopalan M, Josien H, Haggmann WK, *et al.* (2017). Design and Synthesis of Novel, Selective GPR40 AgoPAMs. *ACS medicinal chemistry letters* **8**(2): 221-226.

Pocai A (2012). Unraveling oxyntomodulin, GLP1's enigmatic brother. *The Journal of endocrinology* **215**(3): 335-346.

Rankovic Z, Brust TF, Bohn LM (2016). Biased agonism: An emerging paradigm in GPCR drug discovery. *Bioorganic & medicinal chemistry letters* **26**(2): 241-250.

Rasmussen SG, DeVree BT, Zou Y, Kruse AC, Chung KY, Kobilka TS, *et al.* (2011). Crystal structure of the beta2 adrenergic receptor-Gs protein complex. *Nature* **477**(7366): 549-555.

Rives ML, Vol C, Fukazawa Y, Tinel N, Trinquet E, Ayoub MA, *et al.* (2009). Crosstalk between GABAB and mGlu1a receptors reveals new insight into GPCR signal integration. *The EMBO journal* **28**(15): 2195-2208.

Salahpour A, Espinoza S, Masri B, Lam V, Barak LS, Gainetdinov RR (2012). BRET biosensors to study GPCR biology, pharmacology, and signal transduction. *Frontiers in endocrinology* **3**: 105.

Schroder R, Schmidt J, Blattermann S, Peters L, Janssen N, Grundmann M, *et al.* (2011). Applying label-free dynamic mass redistribution technology to frame signaling of G protein-coupled receptors noninvasively in living cells. *Nature protocols* **6**(11): 1748-1760.

Shapiro H, Shachar S, Sekler I, Hershinkel M, Walker MD (2005). Role of GPR40 in fatty acid action on the beta cell line INS-1E. *Biochemical and biophysical research communications* **335**(1): 97-104.

Siehler S (2007). G12/13-dependent signaling of G-protein-coupled receptors: disease context and impact on drug discovery. *Expert opinion on drug discovery* **2**(12): 1591-1604.

Sivertsen B, Lang M, Frimurer TM, Holliday ND, Bach A, Els S, *et al.* (2011). Unique interaction pattern for a functionally biased ghrelin receptor agonist. *The Journal of biological chemistry* **286**(23): 20845-20860.

Srivastava A, Yano J, Hirozane Y, Kefala G, Gruswitz F, Snell G, *et al.* (2014). High-resolution structure of the human GPR40 receptor bound to allosteric agonist TAK-875. *Nature* **513**(7516): 124-127.

Stoddart LA, Smith NJ, Milligan G (2008). International Union of Pharmacology. LXXI. Free fatty acid receptors FFA1, -2, and -3: pharmacology and pathophysiological functions. *Pharmacological reviews* **60**(4): 405-417.

Tomita T, Masuzaki H, Noguchi M, Iwakura H, Fujikura J, Tanaka T, *et al.* (2005). GPR40 gene expression in human pancreas and insulinoma. *Biochemical and biophysical research communications* **338**(4): 1788-1790.

Yabuki C, Komatsu H, Tsujihata Y, Maeda R, Ito R, Matsuda-Nagasumi K, *et al.* (2013). A novel antidiabetic drug, fasiglifam/TAK-875, acts as an ago-allosteric modulator of FFAR1. *PloS one* **8**(10): e76280.

Yonezawa T, Katoh K, Obara Y (2004). Existence of GPR40 functioning in a human breast cancer cell line, MCF-7. *Biochemical and biophysical research communications* **314**(3): 805-809.

Yuan J, Pandol SJ (2016). PKD signaling and pancreatitis. *Journal of gastroenterology* **51**(7): 651-659.

Yuan J, Slice LW, Rozengurt E (2001). Activation of protein kinase D by signaling through Rho and the alpha subunit of the heterotrimeric G protein G13. *The Journal of biological chemistry* **276**(42): 38619-38627.

## **Footnotes**

This research was supported by Janssen, Pharmaceutical companies of Johnson & Johnson.

## **Conflict of interest:**

The authors declare no conflict of interest.

**Send reprint request to:** Dr. Marie-Laure Rives, Molecular and Cellular Pharmacology, Janssen, Pharmaceutical companies of Johnson & Johnson, 3210 Merryfield Road, San Diego, CA 92121,  
Phone: 858-320-3494  
Email: [mrives1@its.jnj.com](mailto:mrives1@its.jnj.com)

## Figure Legends

**Figure 1: Identification of a new full hGPR40 agonist, Compound A, at the Gαq/IP1/calcium pathway.** A. Structure of Compound A. B. Calcium signaling in a CHO-K1 cell line stably expressing hGPR40. Compound A showed similar efficacy to AM-1638, previously reported as a highly efficacious hGPR40 full agonist and fasiglifam was only partially efficacious. Data presented are representative of three independent experiments performed in quadruplicate for each compound. Data are represented as averages  $\pm$  S.E.M. C. In a CHO-K1 cell line stably expressing hGPR40, Compound A was a full agonist at the IP1 pathway, with similar efficacy as AM-1638. Fasiglifam was a partial agonist with about 50% efficacy ( $50.9 \pm 1.2\%$ ;  $p < 0.0001$ ) compared to Compound A and AM-1638. Data presented are representative of three independent experiments performed in quadruplicate for each compound. Data are represented as averages  $\pm$  S.D. Statistical significance was determined by one-way ANOVA with Dunnett post hoc analysis using GraphPad Prism 7.0 (GraphPad Software, Inc., La Jolla, CA, 92037, USA).

**Figure 2: Compound A is fully efficacious at potentiating GSIS in human islets.** All donors tested were responsive to 12 mM glucose and non-glucose dependent insulin secretagogues, KCl or Glibenclamide. A. In the presence of 12 mM glucose, Compound A significantly potentiated insulin secretion compared to islets treated with glucose alone. The potentiation observed with fasiglifam was  $22.4 \pm 6\%$  ( $p < 0.0001$ ) of the potentiation induced by Compound A. B. In presence of low glucose (2 mM), fasiglifam was not able to potentiate GSIS. Stimulation with Compound A led to a significant potentiation of insulin secretion but at higher concentrations than in presence of high glucose. Data are represented as averages  $\pm$  S.E.M. from 3 different islets. Donors are

different between graphs A and B. Statistical significance was determined by one-way ANOVA with Dunnett post hoc analysis using GraphPad Prism 7.0 (GraphPad Software, Inc., La Jolla, CA, 92037, USA).

**Figure 3: Compound A is a full agonist at  $G\alpha_q$  and  $G\alpha_i2$  and engages the  $G\alpha_{12}$  pathway. A.**

B. and C. Bioluminescence resonance energy transfer (BRET)-based biosensor assays were used to directly monitor G protein activation following GPR40 agonist treatment. A.  $G\alpha_q$  sensor. Compound A and AM-1638 were full agonists at the  $G\alpha_q$  pathway with similar efficacy as  $\alpha$ -linolenic acid. Fasiglifam was a partial agonist with about 40% efficacy compared to Compound A. B.  $G\alpha_i2$  sensor. Compound A and AM-1638 were highly efficacious agonists at the  $G\alpha_i2$  pathway with  $82.5 \pm 4.6\%$  and  $91.6 \pm 4.5\%$  efficacy compared to  $\alpha$ -linolenic acid, respectively. Fasiglifam was a partial agonist at  $G\alpha_i2$  with about 40% efficacy ( $43.5 \pm 2.0\%$ ;  $p < 0.0001$ ) compared to Compound A. C.  $G\alpha_{12}$  sensor. While fasiglifam was inactive at  $G\alpha_{12}$ , Compound A and AM-1638 induced activation of the  $G\alpha_{12}$  protein similarly to the ghrelin receptor (Supplemental Figure 2B) (Evron *et al.*, 2014; Sivertsen *et al.*, 2011). Symbols represent the mean  $\pm$  S.E.M from at least three independent experiments performed in duplicates.

**Figure 4: Compound A and AM-1638 only weakly activate the  $G\alpha_s$ /cAMP pathway. A.**

BRET-based  $G\alpha_s$  biosensor was used to directly monitor  $G\alpha_s$  protein activation following GPR40 agonist treatment. In cells transfected with the glucagon-like peptide 1 (GLP-1) receptor, a well-known  $G\alpha_s$ -coupled receptor, GLP-1[7-36] induced a strong  $G\alpha_s$  response. In hGPR40-transfected cells, Compound A, AM-1638 and  $\alpha$ -linolenic acid only induced a very weak response and fasiglifam was inactive. B. In hGPR40-expressing cells, fasiglifam was inactive at inducing

increases in cAMP production and Compound A and AM-1638 only weakly activated the cAMP pathway compared to the forskolin control performed in the same cells. Data presented are representative of three independent experiments performed in quadruplicate for each compound. Data are represented as averages  $\pm$  S.D.

**Figure 5: Compound A, AM-1638 and fasiglifam potentiate  $\alpha$ -linolenic acid-induced coupling to  $G\alpha_q$  and  $G\alpha_i2$ .** A. and B. Bioluminescence resonance energy transfer (BRET)-based biosensor assays were used to directly monitor G protein activation following GPR40 agonist treatment. A.  $G\alpha_q$  sensor. Compound A, AM-1638 and fasiglifam potentiated an  $EC_{20}$  of  $\alpha$ -linolenic acid at inducing  $G\alpha_q$  coupling to hGPR40. B.  $G\alpha_i2$  sensor. Compound A, AM-1638 and fasiglifam potentiated an  $EC_{20}$  of  $\alpha$ -linolenic acid at inducing  $G\alpha_i2$  coupling to hGPR40. For each compound, data from two independent experiments performed in duplicates were combined and symbols presented are the mean  $\pm$  S.E.M.

**Figure 6: Docking of Compound A in allosteric pocket. A.** Docking of Compound A in the lipid-facing pocket between TM4 and TM5 identified by Lu and colleagues as the allosteric full agonists' binding site. **B.** Ligand: receptor interactions between compound A and hGPR40 predicted from the molecular docking of Compound A into in the lipid-facing pocket identified by Lu and colleagues between TM4 and TM5.

**Figure 7:** Efficacy plot of Compound A, AM-1638 and fasiglifam at multiple G proteins compared to  $\alpha$ -linolenic acid: [ $\log$  scale base 5( $E_{max}$  compound/ $E_{max}$   $\alpha$ -linolenic acid)].

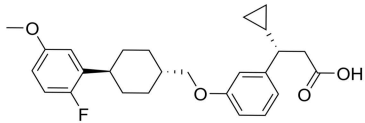
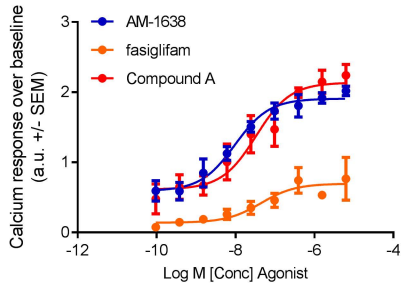
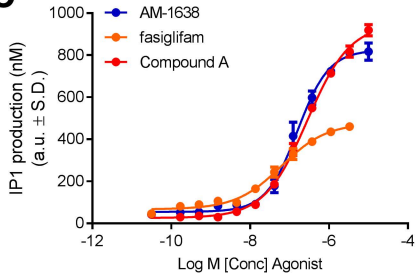
TABLE 1

Potency (EC <sub>50</sub> ) and efficacy relative to α-linolenic acid (E <sub>max</sub> , % of α-linolenic acid ± SD) of fasiglifam, Compound A and AM-1638 at multiple G proteins using BRET-based sensors				
G-protein	E <sub>max</sub> , EC <sub>50</sub> and Hill Slope	fasiglifam	Compound A	AM-1638
Gq	E <sub>max</sub> (% α-linolenic acid)	40.9 ± 4.4 ‡	112.8 ± 5.6	115.2 ± 2.9
	EC <sub>50</sub> (nM) (average ± SD)	8.3 ± 2.2 ‡	0.55 ± 0.03	1.9 ± 0.3
	Hill Slope, average (95% CI)	0.9 (0.5-1.5)	2.3 (1.7-4.4)	1.6 (1.3-2.1)
G11	E <sub>max</sub> (% α-linolenic acid)	35.8 ± 4.4 ‡	122.7 ± 10.0	111.9 ± 9.4
	EC <sub>50</sub> (nM) (average ± SD)	10.1 ± 4.9 ‡	0.3 ± 0.3	1.1 ± 0.3
	Hill Slope, average (95% CI)	0.5 (0.3-0.8)	2.8 (2.0-6.5)	2.5 (1.7-∞)
G12	E <sub>max</sub> (% α-linolenic acid)	n.a. †	>300	>300
	EC <sub>50</sub> (nM) (average ± SD)	n.a. †	28.7 ± 12.5	83.9 ± 26.5
	Hill Slope, average (95% CI)	n.a. †	0.8 (0.5-1.3)	0.8 (0.6-1.1)
G13	E <sub>max</sub> (% α-linolenic acid)	n.a. †	>200	>200
	EC <sub>50</sub> (nM) (average ± SD)	n.a. †	209 ± 105	154 ± 96
	Hill Slope, average (95% CI)	n.a. †	1.0 (0.6-2.0)	1.0 (0.6-2.0)
Gs	E <sub>max</sub> (% α-linolenic acid)	n.a. †	N.D. ‡	N.D. ‡
	EC <sub>50</sub> (nM) (average ± SD)	n.a. †	N.D. ‡	N.D. ‡
	Hill Slope, average (95% CI)	n.a. †	N.D. ‡	N.D. ‡
Gi2	E <sub>max</sub> (% α-linolenic acid)	43.5 ± 2.0 ‡	82.5 ± 4.6	91.6 ± 4.5
	EC <sub>50</sub> (nM) (average ± SD)	4.2 ± 1.0	7.2 ± 1.8	38.0 ± 9.3
	Hill Slope, average (95% CI)	1.2 (0.9-1.6)	1.1 (0.8-1.5)	1.0 (0.8-1.2)
GoB	E <sub>max</sub> (% α-linolenic acid)	n.a. †	72.9 ± 4.5	81.7 ± 5.9
	EC <sub>50</sub> (nM) (average ± SD)	n.a. †	69.9 ± 84.1	277 ± 122
	Hill Slope, average (95% CI)	n.a. †	0.7 (0.5-1.0)	0.6 (0.5-0.9)
Gz	E <sub>max</sub> (% α-linolenic acid)	n.a. †	151.5 ± 10.0	148.4 ± 25.6
	EC <sub>50</sub> (nM) (average ± SD)	n.a. †	11.5 ± 4.4	114 ± 58
	Hill Slope, average (95% CI)	n.a. †	0.8 (0.7-0.9)	0.7 (0.6-0.9)

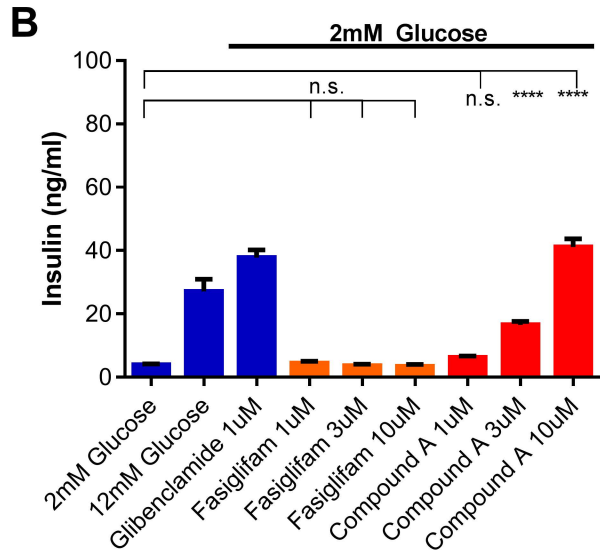
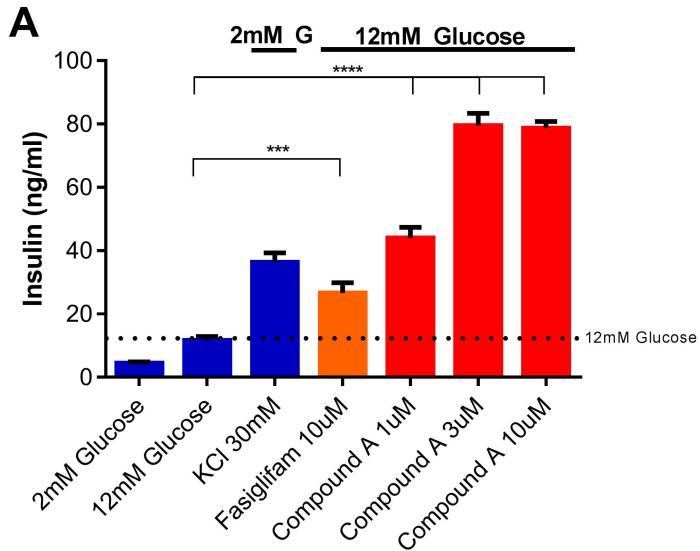
† n.a. not applicable (EC<sub>50</sub> > 50 μM and/or E<sub>max</sub> < 10)

‡ N.D. Not Determined

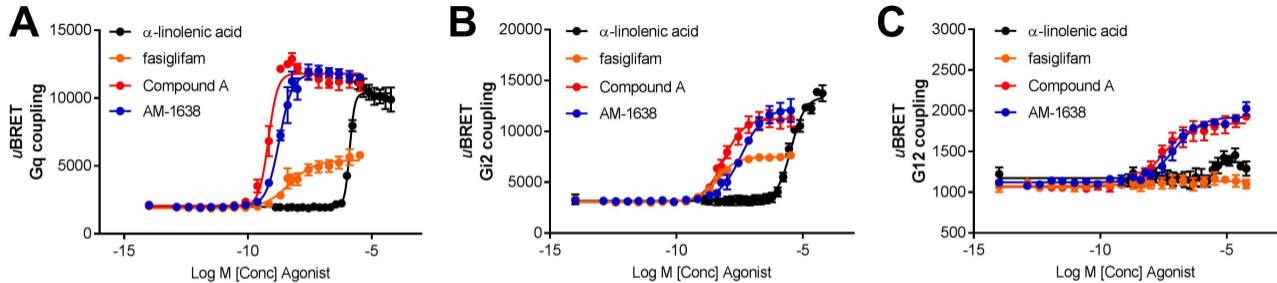
‡ Significantly different from that of Compound A and AM-1638 (p < 0.05)

**A****B****C****Figure 1**

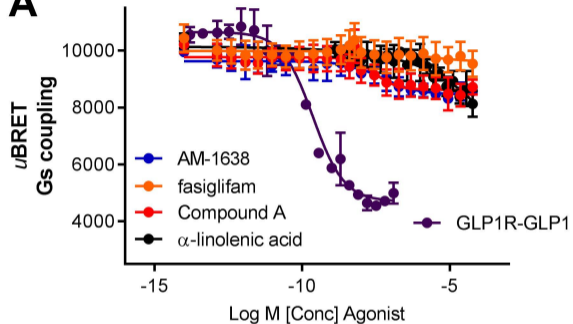
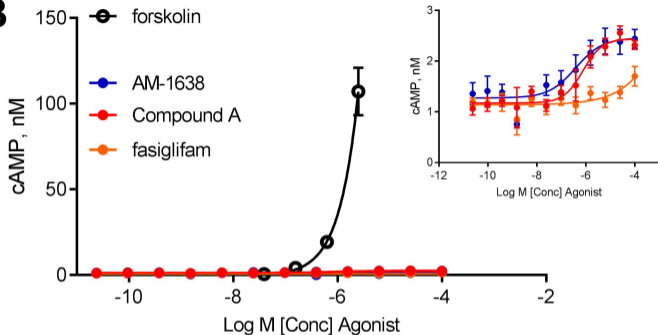


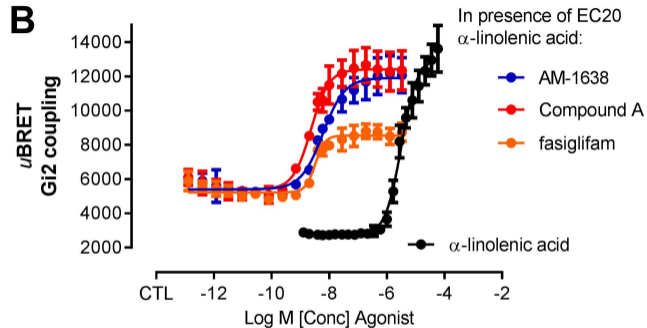
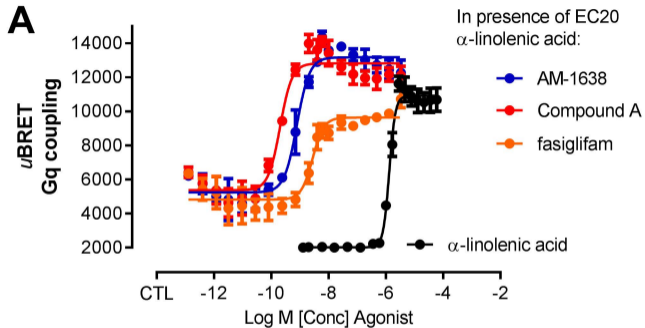


**Figure 2**

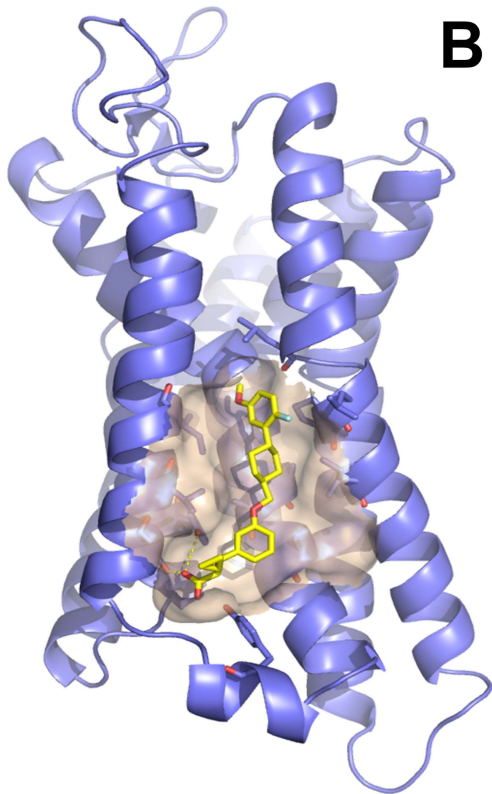
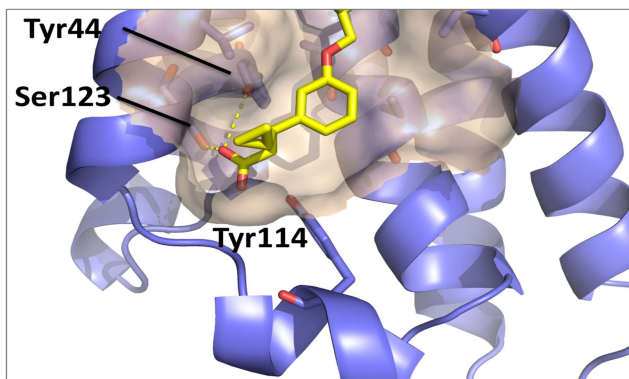
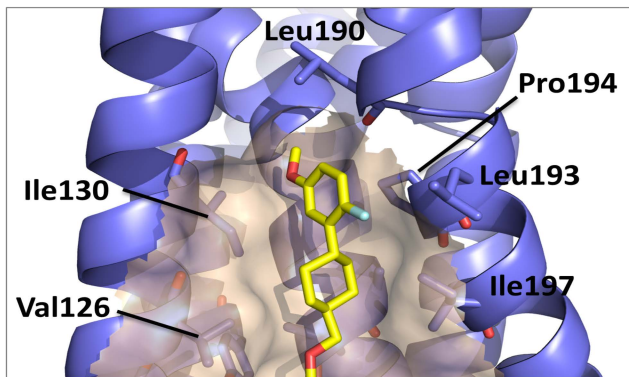


**Figure 3**

**A****B****Figure 4**



**Figure 5**

**A****B****Figure 6**

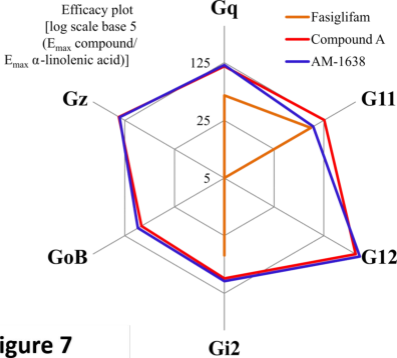


Figure 7